



Alexandru-Gabriel Pielmuş*, Dennis Osterland, Michael Klum, Timo Tigges, Aarne Feldheiser, Oliver Hunsicker and Reinhold Orglmeister

Correlation of arterial blood pressure to synchronous piezo, impedance and photoplethysmographic signal features

Investigating pulse wave features and transit times

Abstract: In this paper we investigate which pulse wave pick-up technologies are well suited for blood pressure trend estimation. We use custom built hardware to acquire electrocardiographic, applanation-tonometric, photo- and impedance-plethysmographic signals during low intensity workouts. Beat-to-beat features and pulse wave runtimes are correlated to the reference arterial blood pressure. Temporal lag adjustment is performed to determine the latency of feature response. Best results are obtained for systolic arterial blood pressure. These suggest that every subject has a range of well-performing features, but it is not consistent among all. Spearman Rho values reach in excess of 0.8, with their significance being validated by p-values lower than 0.01.

Keywords: arterial blood pressure trend, correlation, features, pulse transit time, pulse arrival time, photoplethysmography, vascular impedance, peripheral applanation, non-invasive, continuous, wavelet.

<https://doi.org/10.1515/cdbme-2017-0158>

1 Introduction

As the wearables and biomedicine fields intertwine, the need to reliably, unobtrusively and accurately acquire

bioparameters in ambulatory and stationary settings is on the rise. The arterial blood pressure (ABP) is an important parameter describing the human physiology, yet is difficult to pick up; finding robust alternatives is therefore paramount.

Using peripheral applanation tonometry (pAT), vascular impedance- and photo-plethysmographic (vIPG, PPG) transducers [1], we evaluate whether this combination can be applied to estimate systolic, mean and diastolic ABP trends.

In a precursory publication we have investigated the dependency of the pulse arrival and transit time (PAT, PTT) on the ABP, with results suggesting that PTT is a more reliable indicator for changes thereof [2]. However, the proposed method relied on the use of a reflective PPG sensor, whose signal quality was heavily influenced by sensor positioning, movement and skin composition of the subjects. As such, other more reliable and easily applicable pulse wave transducers have been developed and tested in the current paper: a piezoceramic pAT and a four-wire AC current injection vIPG sensor. All of the related signals are recorded simultaneously so as to allow for a direct quality comparison regarding ABP tracking capabilities of pulse features extracted therefrom. Other than the similarity and interchangeability of these three signals, we investigate if they can be multimodally used to replicate the results obtained by multiple unimodal signals.

2 Methods


2.1 Hardware

Apart from the reference ABP measurement device, all hardware is part of the in-house, custom-built robust Body Sensor Network (rBSN) [3] of the EMSP Chair at the TU Berlin. All signals are acquired at a sampling rate of 500 samples/s with 12 bits of resolution, and are guaranteed by

***Corresponding Author: Alexandru-Gabriel Pielmuş:** Chair of Electronics and Medical Signal Processing, Technische Universität Berlin, Germany, e-mail: a.pielmus@tu-berlin.de

Dennis Osterland, Timo Tigges, Michael Klum, Reinhold Orglmeister: Chair of Electronics and Medical Signal Processing, Technische Universität Berlin, Germany, e-mail: info@emsp.tu-berlin.de

Aarne Feldheiser, Oliver Hunsicker: Klinik für Anästhesiologie m.S. operative Intensivmedizin, Charité Universitätsmedizin Berlin, Germany, e-mail: aarne.feldheiser@charite.de, oliver.hunsicker@charite.de

Open Access. © 2017 Alexandru-Gabriel Pielmuş et al., published by De Gruyter.  This work is licensed under the Creative Commons Attribution-NonCommercial-NoDerivatives 4.0 License.

design to be synchronous within 100 μ s. Data are stored on micro SD cards aboard each sensor node in the network.

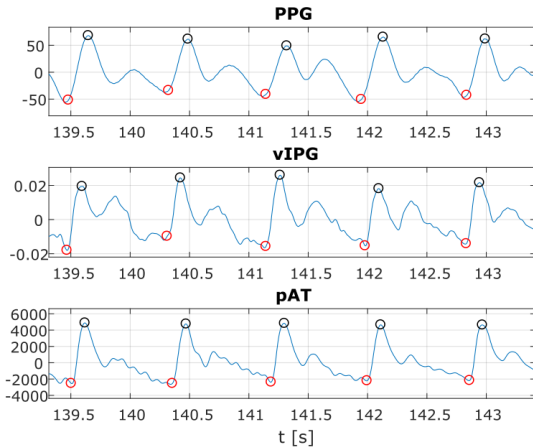


Figure 1: Exemplary recorded pulse waves (Axes unscaled).

The ECG is measured via a simple discrete circuit, built around the INA333 differential amplifier. The analogue bandwidth ranges from 0.5 to 100 Hz. Three leads are measured. The front-end has active as well as passive driven right leg (DRL) capability, depending on requirements. The PPG is recorded by a transmissive finger clip, which has an analogue bandwidth spanning 0.1 to 50 Hz. The DS1843 is the central IC of the three parallel channels for red, infrared and ambient light. The pAT sensor consists of a piezoceramic lead zirconate - lead titanate transducer, with corresponding processing circuitry appended. It is designed to be placed on any location where palpation of a pulse is possible. The vIPG system is of four wire, AC current injection type [4]. It expands the AD5933 IC by a single-ended, improved Howland current pump and a transimpedance amplifier. Nominal peak-to-peak current output is limited to 0.9 mA and a frequency of 10 to 100 kHz. The ABP is measured by a commercially available Omron M10-IT automatic cuff sphygmomanometer. Depending on cuff application and subject BP, a single measurement takes approximately 30 seconds. Pulse waveform excerpts from the sensors are depicted in **Figure 1**.

2.2 Methodology

Ten healthy, young subjects (four female, six male - aged 26.5 ± 3.3 years) were included for testing. The measurement protocol was designed to provoke moderate changes in ABP so as not to overly corrupt the biosignals and interfere with the reference sphygmomanometer [5]. The twelve minute sequence was as follows: 90 seconds rest, 30 s voluntary respiratory arrest, 120 s rest and 60 s light pedalling on a stationary bicycle concluded by a 420 s rest period. ABP was

punctually sampled at six predefined key moments: s60, s110, s210, s300, s420, s600. As this is a highly dynamic process, ABP progression is only roughly foreseeable - an exemplary ABP curve is shown in **Figure 2**. It was attempted to keep the subject upper body as steady as possible throughout the whole procedure, hence the testing was done

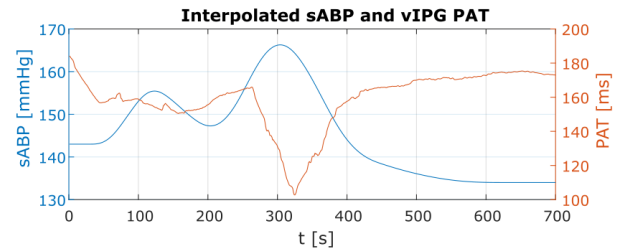


Figure 2: ABP curve plotted alongside feature curve

in a seated position with the left arm resting on a table, slightly below heart level.

The experimental setup consisted of synchronous recording of the following on the left arm: a standard 3-lead Einthoven ECG mounted on the torso; peripheral applanation tonometry on the arteria radialis, mounted with a tourniquet on the inner wrist; vascular impedance plethysmography on the inner side of the elbow; and lastly, transmissive PPG at the index finger. For sake of not interfering with the vIPG current injection, the DRL of the ECG front end is set to passive mode, i.e. half of the operating voltage. vIPG frequency was set to 58 kHz, mean sensing electrode distance was 20 cm for men and 10 cm for women. ABP measurements were acquired by the Omron automatic cuff sphygmomanometer on the right arm.

2.3 Signal processing

Each of the ten datasets lasts for approximately 12 minutes and encompasses roughly 700 valid heartbeats, for a total of over 21000 analysed pulse waveforms. Mathworks Matlab 2017a is used for all signal processing.

The first step is pre-filtering the data, so as to be able to reliably identify fiducial points. For the pAT data, an extra step needs to be performed beforehand, as the raw signal is the differential of the sensed pressure; offset removal and integration via the trapezoidal method are therefore applied. All pulse wave data is then low pass filtered to 5 Hz with a FIR filter, and the baseline is removed by subtracting a 2 s moving average filtered version of the input. ECG data is low pass filtered to 25 Hz and the same baseline removal is applied. Alternatively, a continuous wavelet transform with a 0.1 s wide Mexican Hat wavelet can be performed on all raw input pulse waveforms. This acts approximately as a selective bandpass filter, and yields better noise and interference

rejection at the cost of potential loss of morphological accuracy.

Next, pulse wave data is run through a peak and onset detection algorithm based on Zong [6]. ECG R-peak detection is done by a modified Pan-Tompkins algorithm [7]. The features computed thereupon are enumerated in **Table 1**. Computationally inexpensive features have been specifically chosen and evaluated so as to allow future online signal processing on embedded platforms [8].

Table 1: Used morphological and temporal pulse wave features.

Reference Data	Morph. Features	Temp. Features
Systolic ABP	Pulse height	Pulse arrival time
Mean ABP	Pulse upslope duration	Pulse transit time
Diastolic ABP	Pulse upslope gradient	
	Pulse upslope area	
	Pulse downslope area	
	Pulse up/down area ratio	

The PAT / PTT are defined as the time a pulse wave takes to travel from the heart / any upstream arterial location to the pickup location [9]. The R-peak is chosen as the start fiducial for PAT. To minimize jitter from imprecise onset or peak pulse wave fiducials, the 50% point on the upslope is used. PTT is computed between all of the three pulse waves of **Figure 1**.

For the computation of the area under the pulse curve, a piecewise cubic interpolation is performed on the onset fiducials, and then subtracted from the original. Thus all onsets are aligned to zero amplitude, and the curve areas can be easily integrated numerically.

Due to the intrinsically different temporal locations of the feature samples, a common time base needs to be generated. This is done by interpolating all curves to the time points of the PPG onsets. Because the ABP signal is of low frequency, all interpolated data are filtered and then

downsampled to 1 Hz. Additionally, a 60 s window width moving average filter is applied thereafter.

As varying latencies between change in ABP and feature expression are to be expected, the temporal lag between reference and processed feature waveform is computed and adjusted for, before performing the final correlation. This is achieved by defining a ± 90 s window within whose bounds a cross correlation is performed. The time offset at peak correlation is then asserted.

The correlation of the lag-compensated features to the reference ABP (systolic, mean and diastolic) was evaluated by computing the Spearman Rho, Kendall Tau and Pearson linear coefficient, as well as their corresponding p-values. As it is the most tolerant toward outliers and non-linearity, and the data is most certainly prone to exhibit both these features, the Spearman correlation coefficient should be most relevant.

3 Results

Beginning with the first results, it quickly became apparent that none of the selected features would appropriately correlate to the diastolic blood pressure (BP). **Figure** shows initial results of the correlation analysis, with no lag adjustment or rectification before summation over all datasets. For the systolic ABP, vIPG pulse height and the ratio of PPG up-/downslope area exhibit Spearman and Pearson correlation coefficients between 0.45 and 0.5, with significances of 0.05 down to 0.0005. The PAT from vIPG shows -0.5 to -0.55 correlation, at a significance of around 0.005.

Compensating for the fact that, as apparent from the individual correlation patterns in **Figure**, the sign of the coefficients can switch between subjects, the absolute values

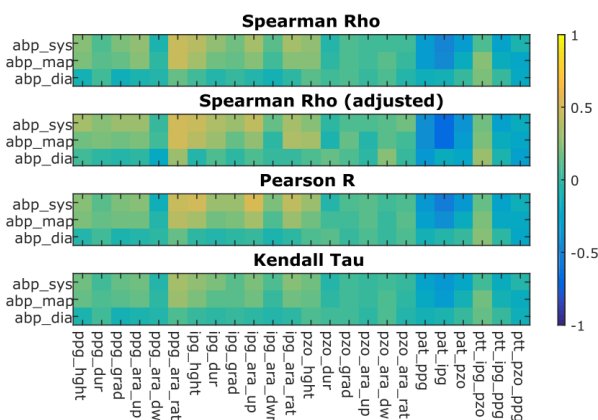


Figure 3: Mean correlation of features to ABP.

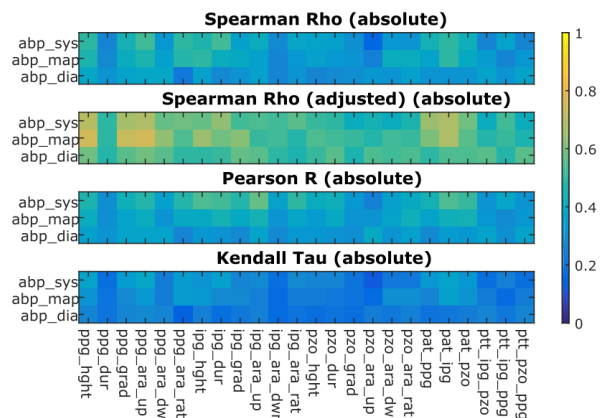


Figure 4: Absolute correlation of features to ABP

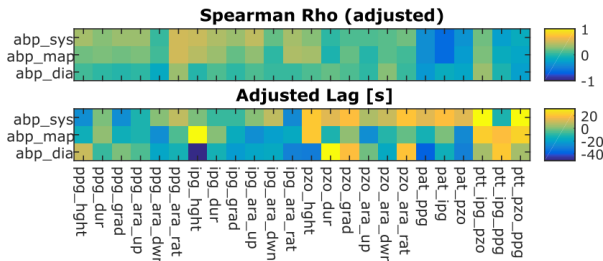


Figure 5: Spearman correlation after lag adjustment.

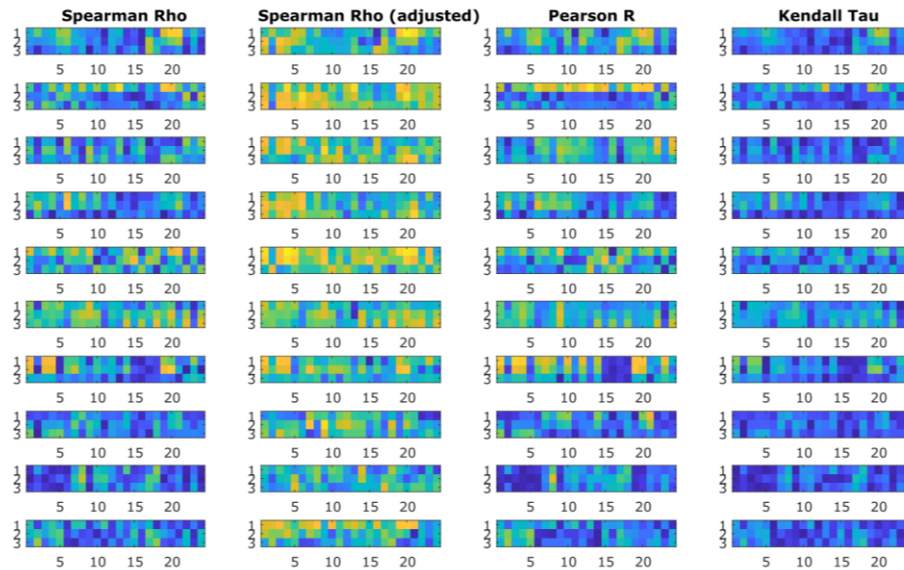


Figure 6: Individual correlation data.

of the data are computed before summation. This yields the results in **Figure**, which are only slightly (0-5%) improved.

The last step, lag compensation, can be seen in both **Figure** and **Figure** as ‘adjusted’. This significantly improves correlation figures (the PAT of vIPG and PPG now range from 0.6 to 0.7 for both systolic and mean ABP) and introduces new promising features such as PPG height, upslope gradient and area. For mean ABP (MAP), Rho values of 0.7 to 0.75 are achieved for these features. Also, some positive lags (warm tones, indicating precedence of the feature to ABP) appear in **Figure** – some being as large as 30 s.

4 Conclusion

In this paper we have investigated which features extracted from pulse waves acquired by PPG, pAT and vIPG are suitable candidates for blood pressure trend estimation. After performing lag compensation, PAT of PPG and vIPG as well as upslope features of PPG have generated the best results. Future work should focus on the combination of these

features so as to obtain more consistent results between subjects.

As can be gathered from **Figure**, individuals exhibit significantly better correlation results (even exceeding 0.9 at extremely low p-values) when compared to the group mean. This seems to stem from the fact that no one feature seems to be performing consistently throughout the experiment.

A possible reason why PAT performs better than PTT in this setup, is the heterogeneity of sensors – this would

indicate that the PAT of differently acquired signals (PPG, vIPG, pAT) fluctuate differently and are not suited for computing the PTT.

Author’s Statement

Research funding: The author state no funding involved. Conflict of interest: Authors state no conflict of interest. Informed consent: Informed consent has been obtained from all individuals included in this study. Ethical approval: The research related to human use complies with all the relevant national regulations, institutional policies and was performed in accordance with the tenets of the Helsinki Declaration, and has been approved by the authors' institutional review board or equivalent committee.

References

- [1] W. Nichols et al. “McDonald’s blood flow in arteries: theoretical, experimental and clinical principles” CRC press, 2011.
- [2] A. Piemuş et al. “Novel computation of pulse transit time from multi-channel PPG signals by wavelet transform” Current Directions in Biomedical Engineering 2016; 2(1).
- [3] M. Pflugradt et al., “Multi-modal signal acquisition using a synchronized wireless body sensor network in geriatric patients” Biomedical Engineering, vol. 60, 2015.

- [4] A. E. Hoetink et al. "On the flow dependency of the electrical conductivity of blood," *IEEE Transactions on Biomedical Engineering*, vol. 51, no. 7, pp. 1251-1261, July 2004.
- [5] J. Muehlsteff et al. "Cuffless Estimation of Systolic Blood Pressure for Short Effort Bicycle Tests: The Prominent Role of the Pre-Ejection Period" 2006 International Conference of the IEEE Engineering in Medicine and Biology Society, New York, NY, 2006, pp. 5088-5092.
- [6] W. Zong et al. "An open-source algorithm to detect onset of arterial blood pressure pulses" *Computers in Cardiology*, 2003. IEEE, 2003. pp. 259-262.
- [7] J. Pan et al. "A Real-Time QRS Detection Algorithm," *IEEE Transactions on Biomedical Engineering*, vol. BME-32, no. 3, pp. 230-236, March 1985.
- [8] X. F. Teng et al. "Continuous and noninvasive estimation of arterial blood pressure using a photoplethysmographic approach" *Proceedings of the 25th Annual International Conference of the IEEE Engineering in Medicine and Biology Society*, 2003, pp. 3153-3156 Vol.4.
- [9] D. Buxi et al. "Blood Pressure Estimation Using Pulse Transit Time From Bioimpedance and Continuous Wave Radar" *IEEE Transactions on Biomedical Engineering*, vol. 64, no. 4, pp. 917-927, April 2017.